Supporting Information

Investigating the reactivity and cellular interactions of indazole-based ruthenium(II) complexes in cancer and leishmania cells

Danilo Kleber Santos Sales,*[a] Gabriela Cruz Fernandes,[b] Carlos Daniel Silva da Silva,[b] Isabela Santos Cezar,[c] Dahara Keyse Carvalho Silva,[d] Milena Botelho Pereira Soares,[d,e] Cássio Santana Meira[c,d,e], Eduardo Henrique Silva de Sousa[f]; Luiz Gonzaga de França Lopes[f] and Denise Santos de Sá [c]

.

[a] *Department of Engineering, Jorge Amado University Center, Salvador, Bahia, Brazil.*
[b] *Department of Chemistry, Federal Institute of Bahia, Salvador, Bahia, Brazil.*
[c] *Department of Life Sciences, State University of Bahia, Salvador, Bahia, Brazil.*
[d] *Gonçalo Moniz Institute, Oswaldo Cruz Foundation, FIOCRUZ, Salvador, Bahia, Brazil.*
[e] *Institute of Innovation in Advanced Health Systems (ISI SAS), University Center SENAI/CIMATEC, Salvador, Bahia, Brazil.*
[f] *Departamento de Química Orgânica e Inorgânica, Universidade Federal do Ceará, Fortaleza, Ceará, Brazil.*

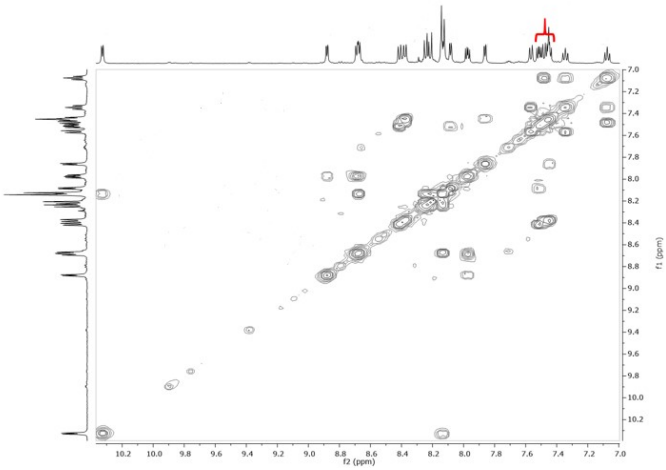

Fig. S1 ^{1}H NMR bidimensional spectrum (*COSY*) of FOR022 and 25 °C, deuterated methanol.

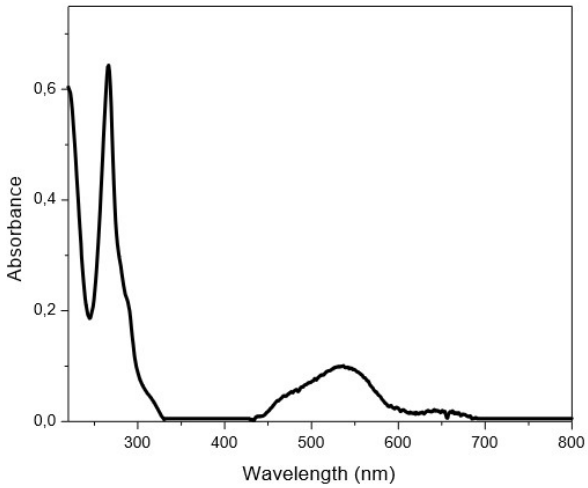

Fig. S2 Electronic absorption spectra of metal complex *cis*-[$RuCl_2(phen)_2$] (FOR020 - precursor) in acetonitrile.

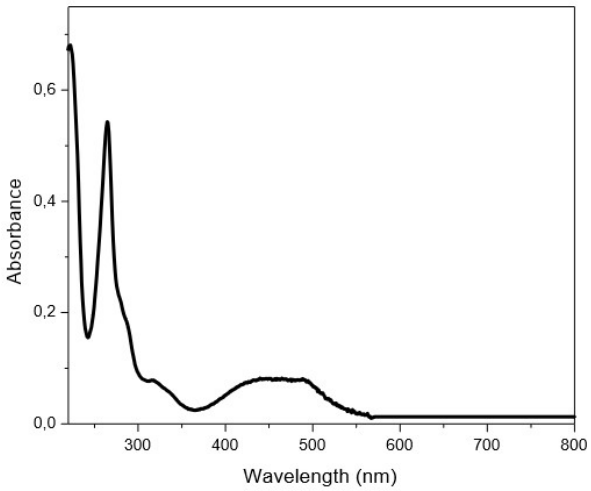

Fig. S3 Electronic absorption spectra of metal complex *cis*-[$RuCl(Hind)(phen)_2$]PF_6 (FOR022) in acetonitrile.

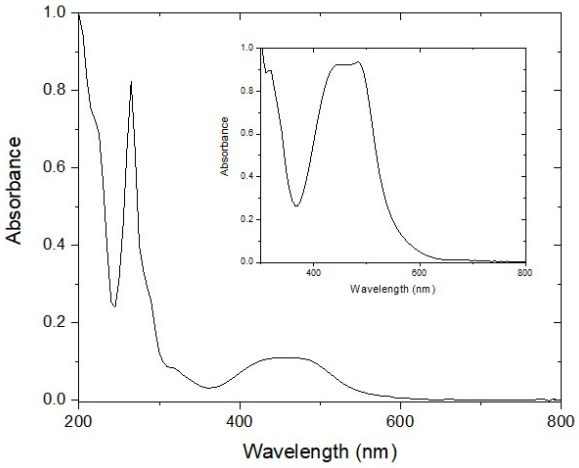

Fig. S4 Electronic absorption spectra of metal complex *cis*-[Ru(Hind)$_2$(phen)$_2$](PF$_6$)$_2$ (FOR0E2), in acetonitrile.

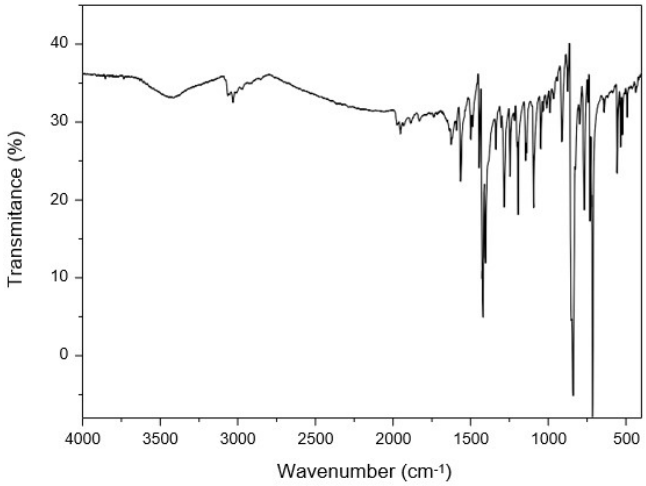

Fig. S5 infrared spectra of metal complex *cis*-[RuCl$_2$(phen)$_2$] (FOR020 - precursor) in KBr pellet.

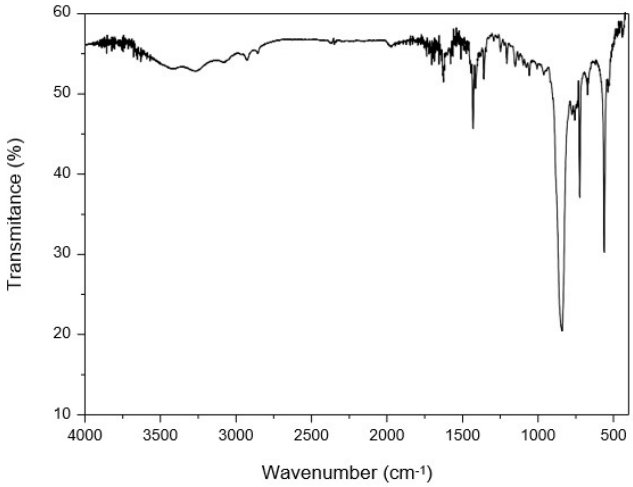

Fig. S6 infrared spectra of metal complex *cis*-[RuCl(Hind)(phen)$_2$]PF$_6$ (FOR022) in KBr pellet.

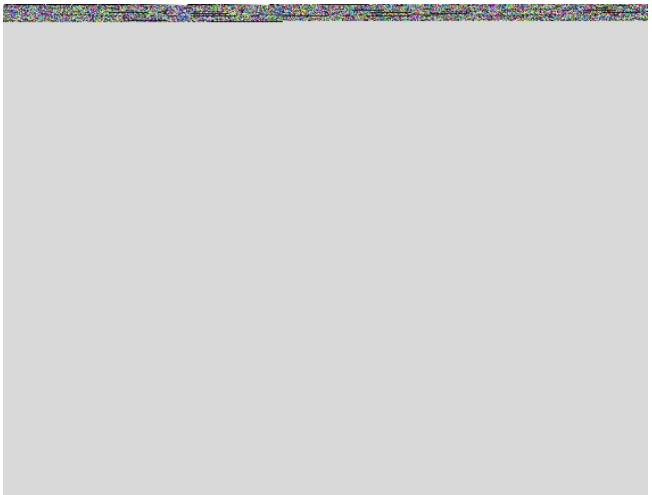

Fig. S7 infrared spectra of metal complex *cis*-[Ru(Hind)$_2$(phen)$_2$](PF$_6$)$_2$ (FOR0E2) in KBr pellet.

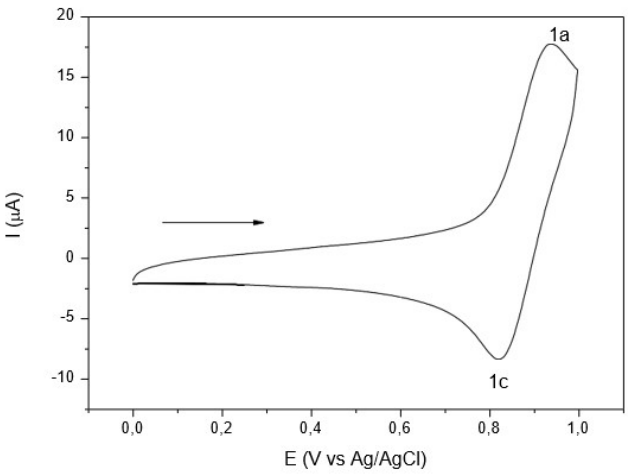

Fig. S8 Cyclic voltammogram of metal complex *cis*-[RuCl(Hind)(phen)$_2$]PF$_6$ (FOR022) (940 μmol L^{-1}) at 25 mV s^{-1} in acetonitrile containing 0.1 mol L^{-1} tetrabutylammonium perchlorate (PTBA). Ferrocene as internal standard, Fc/Fc$^+$ at $E_{1/2}$ = 0.52 V vs. Ag/AgCl - Supplementary data Fig. S10.

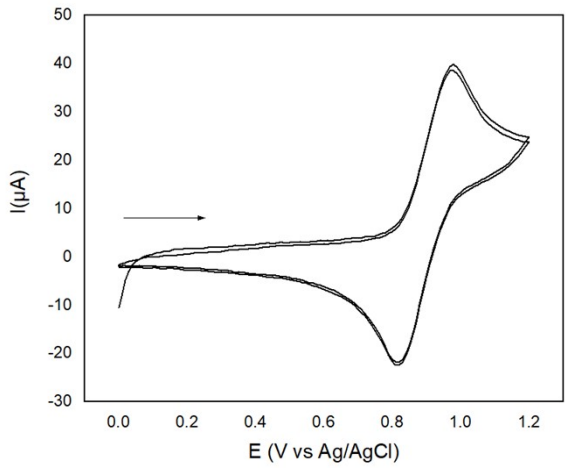

Fig. S9 Cyclic voltammogram metal complex *cis*-[Ru(Hind)$_2$(phen)$_2$](PF$_6$)$_2$ (FOR0E2) (940 µmol L^{-1}) at 25 mV s^{-1} in acetonitrile containing 0.1 mol L^{-1} tetrabutylammonium perchlorate (PTBA). Ferrocene as internal standard, Fc/Fc$^+$ at $E_{1/2}$ = 0.52 V vs. Ag/AgCl - Supplementary data Fig. S10.

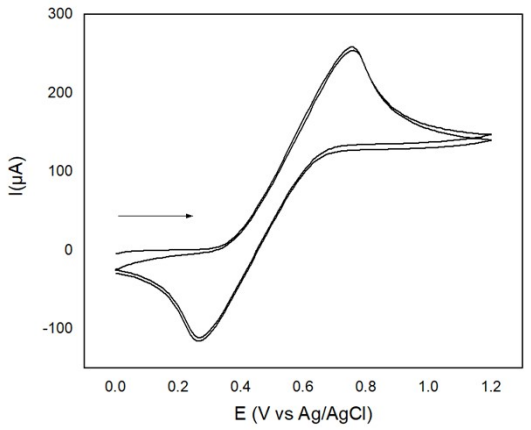

Fig. S10 Cyclic voltammogram of internal standard ferrocene (Fc) in acetonitrile/tetrabutylammonium perchlorate (PTBA). Rate scan: 25 mV s^{-1}.

Table S1 Electrochemical potentials of metal complexes *cis*-[RuCl$_2$(phen)$_2$] (FOR020 - precursor), *cis*-[RuCl(Hind)(phen)$_2$]PF$_6$ (FOR022) and *cis*-[Ru(Hind)$_2$(phen)$_2$](PF$_6$)$_2$ (FOR0E2) in MeCN/PTBA (*vs* Ag/AgCl).

Compounds	Electrochemical potential ($E_{1/2}$) (V)	Experimental λ_{max} (nm) in visible range
	1a/1c	

FOR020	0.47	542
FOR022	0.89	462
FOR0E2	0.87	450